Anomaly Detection in Directed Energy Deposition: A Comparative Study of Supervised and Unsupervised Machine Learning

Berke Ayyıldızlı, Beyza Balota, Kerem Tatari, Shawqi Mohammed Farea, Mustafa Unel
Faculty of Engineering and Natural Sciences
Sabancı University
Istanbul, Turkey
munel@sabanciuniv.edu

***Abstract*—Directed Energy Deposition (DED) is a promising additive manufacturing technology increasingly adopted in critical industries such as aerospace and biomedical applications for fabricating complex metal components. Despite its advantages, maintaining the structural integrity of DED-fabricated parts remains a major challenge due to the occurrence of in-process defects. To address this issue, we propose a data-driven anomaly detection framework for identifying defects using in-situ thermal imaging of the melt pool. Our framework incorporates a range of supervised learning models—including ensemble classifiers and deep neural networks—as well as unsupervised techniques such as autoencoders and clustering algorithms. To enhance model performance, several preprocessing steps were applied, including feature extraction, normalization, and class rebalancing via the Synthetic Minority Oversampling Technique (SMOTE). Experimental results demonstrate the effectiveness of the proposed framework in detecting porosity-related anomalies, achieving an F1 score up to 0.88. These results highlight the strong potential of data-driven anomaly detection models to support real-time quality monitoring and defect detection in metal additive manufacturing processes.**

***Index Terms*—Directed Energy Deposition, Thermal Imaging, Anomaly Detection, Supervised Learning, Unsupervised Learning, Machine Learning**

I. Introduction

Directed Energy Deposition (DED) is a key additive manufacturing process that enables the fabrication and repair of complex metal components layer by layer using a focused energy source. Its flexibility makes it particularly well-suited for high-stakes industries such as aerospace, healthcare, and automotive manufacturing, where mechanical integrity is essential for ensuring safe and reliable operation [1], [2]. Compared to traditional manufacturing techniques, DED facilitates the creation of intricate geometries and enables localized repairs, offering significant advantages in both design flexibility and material efficiency.

Despite these benefits, DED processes are prone to critical in-process defects—most notably porosity, lack of fusion, and cracking—that can degrade the performance and service life of the fabricated parts [3]. Early identification of such defects is essential, especially in applications where structural failure could have catastrophic consequences. Conventional inspection techniques, including manual review and post-process nondestructive evaluation methods such as X-ray Computed Tomography (XCT), are limited by their inability to provide real-time feedback and often require significant time and resources [3], [4]. Additionally, fixed-threshold and rule-based monitoring methods fall short in capturing the complex and transient thermal patterns present in DED processes [4].

In contrast, machine learning (ML) has emerged as a promising approach for real-time, non-invasive defect detection, offering the ability to learn complex and nonlinear relationships from high-dimensional data sources such as thermal imagery [5]. These data-driven methods can generalize across subtle patterns that are difficult to capture using deterministic thresholds or handcrafted rules, making them ideal for DED monitoring. In the existing literature, a variety of supervised ML classifiers have been employed for defect detection, including discriminant analysis, support vector machines, and ensemble methods [6], as well as deep neural network architectures [7]. In addition, unsupervised learning techniques—such as self-organizing maps (SOM), K-means clustering, and DBSCAN (Density-Based Spatial Clustering of Applications with Noise)—have also been explored for identifying anomalies in thermal data during the DED process [8]–[10].

In this study, we introduce a comprehensive framework that leverages both supervised and unsupervised ML techniques to detect porosity-related defects in DED using thermal image data. The unsupervised models include autoencoders and DBSCAN, whilst the supervised models include Random Forest, XGBoost, and Convolutional Neural Networks (CNNs). These models are tested on a dataset comprising 1,564 thermal images of the melt pool, where only 4.7% of images contain porosity-related defects [11]. This severe class imbalance introduces modeling challenges and necessitates preprocessing strategies tailored to noisy, sparse, and imbalanced data. A preprocessing pipeline was implemented to overcome these limitations, including outlier removal, data imputation, normalization, and class rebalancing. Additionally, statistical feature extraction was used to support interpretable models and

reduce input dimensionality. These features included metrics such as mean, standard deviation, skewness, and interquartile range, which have been shown in prior research to correlate with melt pool quality and porosity formation [12].

This work offers a comparative study of ML methods for defect detection in DED, with an emphasis on practical issues such as data imbalance, preprocessing complexity, and model interpretability. By combining domain knowledge with modern ML techniques, the proposed framework aims to advance real-time defect detection in metal additive manufacturing. Ultimately, the results contribute to the goal of establishing DED as a more robust and reliable process for safety-critical industrial applications.

II. Methodology

A. Preprocessing Pipeline

Due to inconsistencies and noise present in the raw thermal image data, a robust preprocessing pipeline was implemented to prepare model-ready inputs and enhance the performance of both supervised and unsupervised learning models.

Some images in the dataset contain zero-valued pixels and/or pixels with missing values. The values of these pixels were imputed using the mean of their respective columns within each image. Then, the thermal data underwent min-max normalization, scaling pixel values to the range of [0, 1]. This normalization step was crucial for stabilizing gradient-based optimizers in neural network training and ensuring consistency and comparability across ML models.

Following normalization, dimensionality reduction and interpretability improvements were achieved through the extraction of statistical features. Each thermal image was transformed into a structured feature vector comprising 11 statistical descriptors: minimum (*Min_Temp*), maximum (*Max_Temp*), mean (*Mean_Temp*), standard deviation (*Std_Temp*), median (*Median_Temp*), first quartile (*Q1*), third quartile (*Q3*), interquartile range (*IQR*), skewness, kurtosis, and peak temperature pixel (*High_Temp_Pixels*). These features effectively summarize the spatial and statistical properties of the melt pool temperature distribution, providing a compact and informative input format for training supervised tree-based classifiers such as Random Forest and XGBoost.

Considering the inherent imbalance in the dataset—with defective images constituting approximately 4.7%—the Synthetic Minority Oversampling Technique (SMOTE) was employed during training the supervised models. SMOTE generates synthetic minority class samples by interpolating between existing anomalous instances, significantly mitigating classification bias and improving the detection recall for rare defects.

Collectively, these preprocessing strategies ensured the dataset's compatibility and consistency across diverse ML models, ultimately enhancing the effectiveness and interpretability of the anomaly detection framework.

B. Supervised ML Models

1) Ensemble Tree-based Models: The ensemble tree-based models include two effective classifiers as follows:

a) Random Forest: It is an ensemble ML algorithm that combines multiple decision trees to deliver robust predictions through majority voting [13]. Random forests are particularly effective in handling high-dimensional data, reducing overfitting, and providing feature importance insights, making them a preferable choice for anomaly detection in DED processes using thermal image-derived features.

b) XGBoost: Extreme Gradient Boosting (XGBoost) [14] is an advanced gradient boosting framework that builds upon traditional tree-based ensemble methods by employing iterative training of shallow decision trees. XGBoost is especially renowned for its performance on structured, tabular datasets and its inherent robustness in managing class imbalance, sparse features, and noisy data, making it particularly suitable for anomaly detection in DED processes.

Both classifiers were configured and fine-tuned to achieve optimal performance while ensuring generalizability. Through preliminary experimentation and cross-validation, the hyperparameters were selected according to Table I, ensuring the best compromise between predictive accuracy and model simplicity. The random state was set at 42 for reproducibility of experimental results.

TABLE I
HYPERPARAMETERS OF RANDOM FOREST AND XGBOOST

Random Forest		**XGBoost**	
Number of Estimators	100	Number of Estimators	100
Max. Depth	5	Max. Depth	3
Min. Samples per Split	5	L2 regularization	1
Min. Samples per Leaf	2	L1 regularization	0.5

For both classifiers, a structured feature vector comprising 11 statistical features extracted from the thermal images was used as input. The dataset was divided into training and test sets using a stratified 70%-30% split, preserving the original class distribution within each subset. The SMOTE algorithm was then applied solely to the training set to avoid data leakage and realistically simulate practical scenarios, resulting in balanced class proportions that enhance the classifier's sensitivity to anomalies.

By leveraging carefully extracted statistical features, robust oversampling techniques, and thorough hyperparameter tuning, these supervised approaches significantly enhances the defect detection process, as can be noticed in Section III.

Lastly, one of the inherent key strengths of Random Forest and XGBoost lies in their transparency regarding feature importance, allowing practitioners to directly interpret and understand critical features impacting anomaly detection outcomes. Consequently, this interpretability is particularly beneficial for manufacturing engineers and quality analysts in pinpointing key indicators of defects in real-world DED processes.

2) Convolutional Neural Network (CNN): CNNs are a subclass of deep learning models, particularly effective for spatial data such as images. In this study, CNNs were utilized in a supervised learning context to directly classify thermal images as either defective or non-defective.

After preprocessing, the dataset was split into training and test sets with an 70%-30% stratified split to preserve class distribution. To address the highly imbalanced nature of the dataset (only $\sim$ 4.7% are defective frames), SMOTE was applied to the training set. Since SMOTE requires 2D inputs, training images were first flattened, oversampled, and reshaped back to their original shape. This significantly improved the model's sensitivity to rare anomaly patterns.

The CNN architecture consisted of the following layers:

- **Conv2D (16 filters)** with ReLU activation and a 3×3 kernel, followed by a maximum pooling layer.
- **Conv2D (32 filters)** with ReLU activation and a 3×3 kernel, followed by a maximum pooling layer
- **Flatten layer** to convert spatial features into a dense vector.
- **Dropout layer (rate = 0.3)** to prevent overfitting.
- **Dense layer (64 units)** with ReLU activation.
- **Output layer (1 unit)** with sigmoid activation for binary classification.

The model was compiled with the Adam optimizer (learning rate = 0.001), using the binary cross-entropy loss. The network was trained for 10 epochs with a batch size of 16, using 20% of the training data as a validation set. As shown in Section III, CNN presents a promising direction for integrating deep learning with real-time quality assurance in DED processes.

C. Unsupervised ML Models

1) Autoencoder: Autoencoders are a type of artificial neural network primarily used for unsupervised learning, particularly anomaly detection tasks. They are designed to learn a compressed, low-dimensional representation of the input data and subsequently reconstruct the input from this encoding. Deviations between the input and reconstructed output serve as a basis for identifying anomalous instances [15].

The model implemented in this study consists of three primary layers: an input, encoding layer, and decoding layer. The input layer accepts flattened vectors of the thermal images. The encoding layer contains 64 neurons, strategically selected through empirical testing to ensure sufficient information retention without overfitting. This layer employs the ReLU activation function because of its efficacy in handling continuous numeric data and mitigating issues such as vanishing gradients. The decoding layer mirrors the dimensionality of the input layer and uses a sigmoid activation function to produce output values within a normalized range of 0 to 1, ensuring compatibility with the scaled thermal image data.

The autoencoder was trained using the entire dataset of preprocessed thermal images, consisting of 1,564 frames, each normalized to manage pixel value disparities. The training regime consisted of 50 epochs with a batch size of 16, determined through preliminary experimentation to balance training performance and computational efficiency. During training, input data points were continuously reconstructed, using the Adam optimizer to minimize the mean square error (MSE) loss between the original and reconstructed frames.

After training, anomaly detection was performed by evaluating the reconstruction error for each thermal frame. The underlying hypothesis is that anomalous frames, characterized by porosity or structural defects, inherently deviate significantly from normal thermal patterns, resulting in a higher reconstruction error. To systematically identify anomalies, two distinct thresholds based on the percentile distribution of reconstruction errors were established:

- **95th percentile threshold**: Frames with MSE above the 95th percentile were flagged as anomalies.
- **99th percentile threshold**: A more conservative approach, identifying only the extreme deviations by setting a threshold at the 99th percentile.

This dual-threshold strategy allowed a nuanced analysis of detection sensitivity and specificity, providing insights into the optimal balance for practical anomaly detection within industrial contexts. Overall, the autoencoder-based anomaly detection methodology outlined provides a robust, unsupervised framework adaptable for monitoring DED processes, offering a valuable alternative when labeled data is scarce or expensive to obtain.

2) DBSCAN: It is a density-based clustering algorithm widely used in unsupervised anomaly detection tasks. Unlike traditional clustering algorithms, DBSCAN does not require a predefined number of clusters; instead, it identifies clusters based on the density of data points, classifying points in low-density regions as anomalies [16]. Given the high-dimensional nature of the thermal images, dimensionality reduction was critical for the effective application of DBSCAN. Principal Component Analysis (PCA) was employed to reduce the dimensionality of the input thermal images to 50 principal components [17]. This transformation significantly decreased computational complexity, improved clustering efficiency, and enhanced the clarity of density-based clusters.

Nonetheless, the optimal parameter selection is essential for DBSCAN performance. The algorithm primarily depends on two parameters: the neighborhood radius (ϵ) and the minimum number of points required to form a dense region (*min_samples*). To determine the optimal ϵ value, a k-distance heuristic method was utilized. Specifically, distances to the 5th nearest neighbor for each data point were calculated, sorted, and plotted to identify an elbow point—representing an optimal balance between overly fragmented clusters (too small ϵ) and merged clusters (too large ϵ). Based on this heuristic, the ϵ value was set to 7.7, while the *min_samples* parameter was set to 5 (see Fig. 1). This configuration provided an effective balance, ensuring that density-based clustering appropriately distinguished anomalies from typical data patterns. With the optimized parameters, DBSCAN clusters the PCA-transformed image data into dense regions, labeling points outside these clusters as anomalies.

III. Results and Discussion

A. Dataset Description

The dataset used in this work [11] consists of 1,564 thermal images of the melt pool recorded during the fabrication

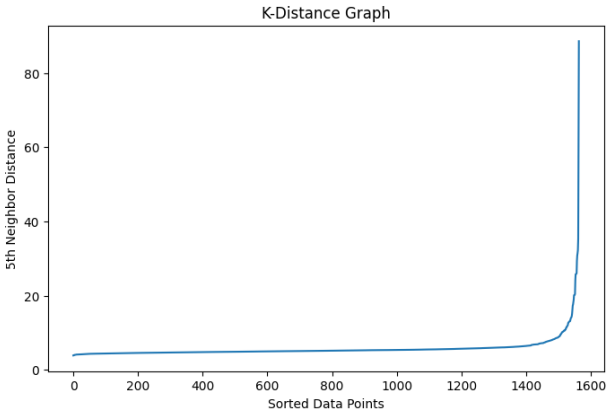

Fig. 1. The K-Distance graph used for optimal epsilon value selection. The sharp increase (elbow) around 7.7 suggests this as the optimal ϵ value.

of Ti–6Al–4V thin-walled structures using the OPTOMEC LENS™ 750 system. The thermal images were captured in-process using a Stratonics dual-wavelength pyrometer, which records a top-down view of the melt pool during laser deposition. Each frame consists of a 200×200 pixel thermal image capturing the relative temperature distribution of the melt pool. Binary porosity labels were assigned based on post-process inspection using Nikon XT H225 X-ray Computed Tomography. Only 74 images (about 4.7%) contain porosity-related defects whilst the remaining 1490 images are defect-free, leading to a significant class imbalance. This remarkable class imbalance poses challenges for model generalization and sensitivity to rare events. Thus, the dataset provides a rich basis for evaluating supervised and unsupervised learning approaches under real-world DED conditions.

B. Defect Detection Results

The comparative evaluation of the models is presented in Tables II and III, with corresponding confusion matrices shown in Figs. 2 and 3. Each model was assessed based on its ability to identify porosity-related anomalies from thermal image data, under the same preprocessing and evaluation.

TABLE II
SUPERVISED MODELS RESULTS

Model	Precision	Recall	F1-Score	Accuracy
CNN	**0.90**	**0.86**	**0.88**	**0.99**
Random Forest	0.86	**0.86**	0.86	0.98
XGBoost	0.89	0.76	0.82	0.98

TABLE III
UNSUPERVISED MODELS RESULTS

Model	Precision	Recall	F1-Score	Accuracy
Autoencoder (99th)	0.75	0.17	0.28	0.96
Autoencoder (95th)	0.54	0.61	0.57	0.96
DBSCAN	0.54	0.52	0.53	0.96

Among the supervised models, the CNN model exhibited the most favorable performance profile. It achieved the most balanced trade-off between precision and recall, and demonstrated minimal misclassification of both normal and defective instances, as reflected in its confusion matrix. The direct use of image-level data, without handcrafted features, likely contributed to its ability to capture nuanced spatial patterns indicative of structural defects.

The ensemble tree-based models yielded good results, although working with low-dimensional input data compared to CNN. In particular, Random Forest achieved results comparable to CNN with an F1 score of 0.86. It yielded consistently high results across all metrics. The confusion matrix for Random Forest reveals only a small number of false positives and false negatives, underscoring its reliability in practical classification tasks. XGBoost, while slightly behind the other two, remained a competitive model with high precision and moderate recall. Its performance suggests that it is more conservative in detecting anomalies, favoring precision over sensitivity. This behavior can be useful in industrial settings where minimizing false alarms is critical, though it may result in some defective instances being overlooked.

In contrast, the unsupervised models demonstrated a wider range of performance, with substantial variation depending on threshold sensitivity and underlying assumptions. The autoencoder's detection capability was heavily influenced by the selected percentile threshold. At the 95th percentile, it captured a larger portion of true anomalies but also introduced more false positives. The 99th percentile threshold, being more conservative, reduced false positives at the expense of significantly lower recall. This trade-off is clearly reflected in the differences between the two confusion matrices in Fig. 3.

DBSCAN, as a clustering-based method, struggled to consistently distinguish defective instances from the background class. Its detection capability was less focused, and it tended to misclassify both normal and anomalous samples. Despite dimensionality reduction via PCA and careful parameter tuning, DBSCAN's density-based assumptions proved less effective in this context, where anomalies are subtle and highly variable.

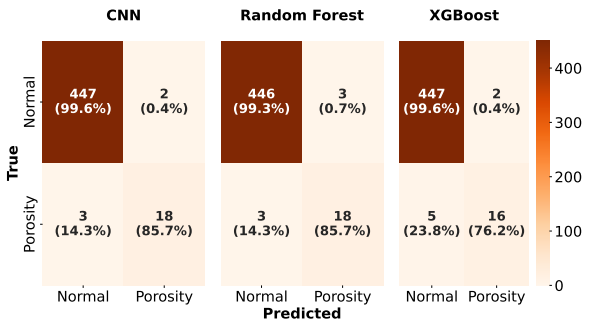

Fig. 2. Confusion matrices of the supervised models.

When comparing the two learning paradigms, supervised models clearly outperformed unsupervised ones across all evaluation criteria. The availability of labeled data and the use of class rebalancing techniques like SMOTE allowed supervised classifiers to develop more discriminative decision

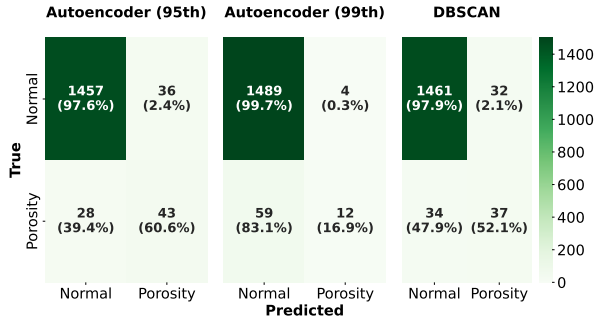

Fig. 3. Confusion matrices of the unsupervised models.

boundaries. In contrast, unsupervised models were constrained by their reliance on reconstruction error or density estimation, which are less sensitive to fine-grained patterns in imbalanced datasets. While autoencoders offered a flexible and scalable detection framework, their effectiveness was tightly coupled to threshold selection, and DBSCAN lacked the granularity needed for precise anomaly identification. These results collectively emphasize the strength of supervised approaches in scenarios where sufficient labeled data is available, and suggest that while unsupervised methods can offer complementary insights, they require careful calibration to reach competitive performance.

C. Feature Analysis

Feature-level analysis revealed several insights into model behavior and predictive performance. To better understand the relationships among input features, a Pearson correlation test was conducted. The correlation matrix, shown in Fig. 4, indicates strong collinearity among central tendency features such as *Mean_Temp*, *Median_Temp*, *Q1*, and *Q3*, suggesting redundancy in the thermal distribution representation. In contrast, features like *Skewness*, *Kurtosis*, and *IQR* demonstrated lower correlation with others, implying they provide orthogonal, potentially more informative cues for anomaly detection.

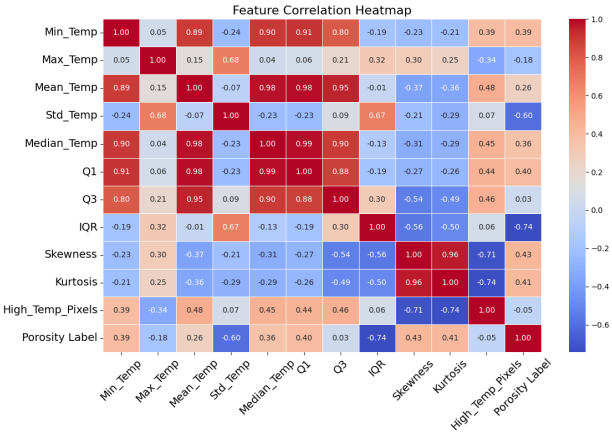

Fig. 4. Feature correlation heatmap among extracted statistical features.

The feature importance rankings derived from supervised models further validate the relevance of specific features. The importance plots for Random Forest and XGBoost are provided in Figs. 5 and 6, respectively. Both Random Forest and XGBoost consistently prioritized *IQR* and *Std_Temp* as the most influential attributes in distinguishing between normal and defective samples. This aligns with the observation that defective frames often display abrupt changes in temperature variance, which are effectively captured by interquartile spread and standard deviation.

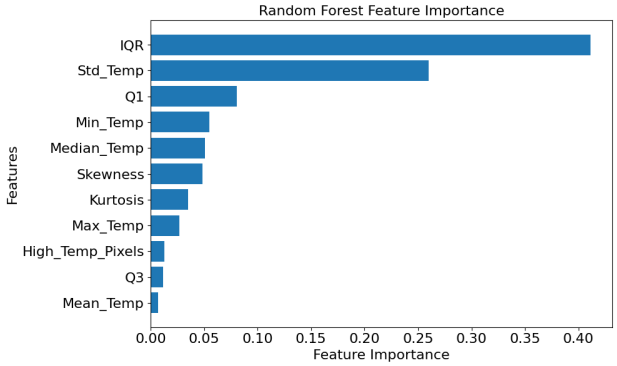

Fig. 5. Feature importance plot from the Random Forest model.

Interestingly, while *Min_Temp* and *Median_Temp* appeared highly correlated in the correlation matrix, their respective importances varied between models—suggesting that although correlated, they do not necessarily provide equivalent discriminative value. This underscores the benefit of ensemble-based feature evaluation, where subtle nonlinear relationships are accounted for during tree construction.

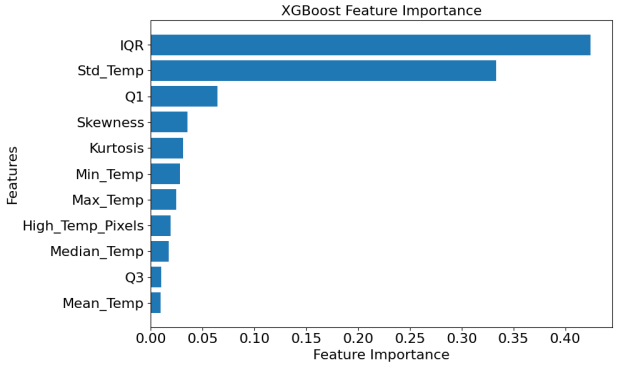

Fig. 6. Feature importance plot from the XGBoost model.

Altogether, the correlation and feature importance analyses offer actionable insights for dimensionality reduction, feature selection, and interpretability. They confirm that a subset of carefully engineered features—particularly those reflecting distribution shape and spread—can effectively support robust classification, even in imbalanced anomaly detection settings.

D. Final Remarks

a) ***Learning paradigm****:* Supervised models clearly benefited from labeled data and class rebalancing techniques, enabling them to achieve higher and more consistent detection accuracy. However, this advantage comes at the cost of

increased data annotation effort and reduced flexibility. In industrial settings where defect annotation is costly or infeasible at scale, the reliance of supervised models on labeled datasets may limit their broader applicability. In contrast, unsupervised models offered greater flexibility by operating without labeled defect data, making them appealing for anomaly detection in exploratory or early-stage quality monitoring systems.

*b) **Threshold Sensitivity and Stability**:* While autoencoders provided a scalable and adaptable framework capable of learning general thermal patterns, their effectiveness was tightly coupled to the choice of reconstruction error threshold. This introduces subjectivity and leads to performance trade-offs—particularly between recall and false-positive rates. Similarly, DBSCAN was highly sensitive to parameter selection (ϵ and *min_samples*) and struggled with the subtle and highly variable defect patterns typical of DED processes.

*c) **Interpretability and Practical Transparency**:* From an interpretability standpoint, the supervised tree-based models – Random Forest and XGBoost – provided clear advantages. Through feature importance rankings, these models enabled traceable classification decisions and gave practitioners direct insights into which statistical temperature features were most indicative of porosity-related anomalies. This level of transparency is particularly valuable in high-stakes manufacturing environments, where model trustworthiness is critical. On the other hand, although unsupervised models are more adaptable, their decisions are often harder to explain—especially when based on latent encodings or density-based assumptions.

*d) **Deployment Considerations**:* While supervised models deliver stronger performance when sufficient labeled data is available, their deployment requires pre-existing defect annotations and careful data balancing. Unsupervised approaches, however, can be rapidly deployed in dynamic environments with limited prior knowledge, making them better suited for initial system integration or ongoing monitoring. The optimal deployment strategy may involve a hybrid approach—utilizing unsupervised methods for continuous monitoring or early anomaly flagging, followed by supervised refinement when annotated data becomes available.

IV. Conclusion

This study presents a comprehensive comparison of supervised and unsupervised learning approaches for anomaly detection in DED processes based on thermal image data, highlighting the respective strengths and limitations of each paradigm. Supervised models—particularly CNN, Random Forest, and XGBoost—consistently outperformed their unsupervised counterparts, benefiting from labeled data, synthetic oversampling via SMOTE, and statistically engineered features. While autoencoders and DBSCAN offered greater flexibility and did not require labeled data, their performance was more sensitive to thresholding and parameter selection.

The results highlight the practicality and reliability of supervised learning in quality-critical applications where labeled datasets are available. However, unsupervised methods remain valuable for early-stage deployment and real-time monitoring scenarios. Moving forward, hybrid frameworks that combine the strengths of both paradigms—starting with unsupervised detection and refining with supervised feedback—offer a promising direction for scalable, interpretable, and robust defect detection in metal additive manufacturing.

References

[1] A. Dass and A. Moridi, "State of the art in directed energy deposition: From additive manufacturing to materials design," *Coatings*, vol. 9, no. 7, p. 418, 2019.

[2] S. H. Li, P. Kumar, and S. Chandra, "Directed energy deposition of metals: Processing, microstructures, and mechanical properties," *International Materials Reviews*, vol. 68, no. 1, pp. 1–44, 2023.

[3] D. Tang, X. He, B. Wu, X. Wang, T. Wang, and Y. Li, "The effect of porosity defects on the mid-cycle fatigue behavior of directed energy deposited Ti–6Al–4V," *Theoretical and Applied Fracture Mechanics*, vol. 118, p. 103296, 2022.

[4] T. Herzog, M. Brandt, A. Trinchi *et al.*, "Defect detection by multi-axis infrared process monitoring of laser beam directed energy deposition," *Scientific Reports*, vol. 14, no. 1, p. 3861, 2024.

[5] H. Gaja and F. Liou, "Defect classification of laser metal deposition using logistic regression and artificial neural networks for pattern recognition," *International Journal of Advanced Manufacturing Technology*, vol. 94, pp. 315–326, 2018.

[6] M. Khanzadeh, S. Chowdhury, M. Marufuzzaman, M. A. Tschopp, and L. Bian, "Porosity prediction: Supervised-learning of thermal history for direct laser deposition," *Journal of Manufacturing Systems*, vol. 47, pp. 69–82, 2018.

[7] D. B. Patil, A. Nigam, S. Mohapatra, and S. Nikam, "A deep learning approach to classify and detect defects in the components manufactured by laser directed energy deposition process," *Machines*, vol. 11, no. 9, 2023.

[8] H. Taheri, L. W. Koester, T. A. Bigelow, E. J. Faierson, and L. J. Bond, "In situ additive manufacturing process monitoring with an acoustic technique: clustering performance evaluation using k-means algorithm," *Journal of Manufacturing Science and Engineering*, vol. 141, no. 4, 2019.

[9] A.-I. García-Moreno, "Automatic quantification of porosity using an intelligent classifier," *International Journal of Advanced Manufacturing Technology*, vol. 105, no. 5, pp. 1883–1899, 2019.

[10] S. M. Farea, M. Unel, and B. Koc, "Defect prediction in directed energy deposition using an ensemble of clustering models," in *Proceedings of the 2024 IEEE 22nd International Conference on Industrial Informatics (INDIN)*, 2024, pp. 1–14.

[11] C. Zamiela, W. Tian, S. Guo, and L. Bian, "Thermal-porosity characterization data of additively manufactured Ti–6Al–4V thin-walled structure via laser engineered net shaping," *Data in Brief*, vol. 51, p. 109722, 2023.

[12] A.-I. García-Moreno, "Automatic quantification of porosity using an intelligent classifier," *International Journal of Advanced Manufacturing Technology*, vol. 105, no. 5, pp. 1883–1899, 2019.

[13] L. Breiman, "Random forests," *Machine Learning*, vol. 45, no. 1, pp. 5–32, 2001.

[14] T. Chen and C. Guestrin, "XGBoost: A scalable tree boosting system," in *Proceedings of the 22nd ACM SIGKDD International Conference on Knowledge Discovery and Data Mining*, San Francisco, CA, USA, 2016, pp. 785–794.

[15] C. Zhou and R. C. Paffenroth, "Anomaly detection with robust deep autoencoders," in *Proceedings of the 23rd ACM SIGKDD International Conference on Knowledge Discovery and Data Mining (KDD)*, 2017, pp. 665–674.

[16] D. Deng, "DBSCAN clustering algorithm based on density," in *Proceedings of the 2020 7th International Forum on Electrical Engineering and Automation (IFEEA)*, Zhuhai, China, 2020, pp. 100–103.

[17] D. J. Hemanth, "Dimensionality reduction of production data using PCA and DBSCAN techniques," *International Journal of Scientific Research in Engineering and Development*, vol. 3, no. 6, pp. 325–329, 2020.